PHYSICAL REVIEW C **83**, 014316 (2011)

Discovery of a 10 μs isomeric state in $^{139}_{63}$Eu

D. M. Cullen,[1] P. J. R Mason,[1,*] C. Scholey,[2] S. Eeckhaudt,[2] T. Grahn,[2] P. T. Greenlees,[2] U. Jakobsson,[2] P. M. Jones,[2] R. Julin,[2] S. Juutinen,[2] S. Ketelhut,[2] A. M. Kishada,[1] M. Leino,[2] A.-P. Leppänen,[2] K. Mäntyniemi,[2] P. Nieminen,[2] M. Nyman,[2] J. Pakarinen,[2,†] P. Peura,[2] M. G. Procter,[1] P. Rahkila,[2] S. V. Rigby,[1,†] J. Sarén,[2] J. Sorri,[2] J. Uusitalo,[2] B. J. Varley,[1] and M. Venhart[2]

[1] *School of Physics and Astronomy, Schuster Laboratory, University of Manchester, Manchester M13 9PL, United Kingdom*

[2] *Department of Physics, University of Jyväskylä, Jyväskylä, FIN-40014 Finland*

(Received 22 September 2010; published 28 January 2011)

Recoil-isomer tagging with the ^{54}Fe + ^{92}Mo reaction was used to establish a 10(2)-μs isomeric state in ^{139}Eu. Prompt versus delayed γ-ray coincidence data have revealed the presence of a prompt rotational band built upon the isomer. The alignment properties of the states in this band show that the isomer is based upon a proton $g_{7/2}$ configuration. The decay of the isomer takes place through a single 26-keV $E1$ transition. The γ-ray transition strength for this decay is consistent with those established in the neighboring isomeric gamma-soft nuclei. In these nuclei, isomers are expected to form as a consequence of differences in nuclear shapes or configurations, and the natural hindrance associated with configuration-changing $E1$ transitions. The isomeric nature of the state in ^{139}Eu is reasoned to be because of difference in shape of the proton $g_{7/2}$ state and the proton $h_{11/2}$ ground state to which it decays.

DOI: 10.1103/PhysRevC.83.014316 PACS number(s): 23.35.+g, 21.10.Re, 23.20.Lv, 27.60.+j

I. INTRODUCTION

Long-lived or isomeric nuclear states are known to exist in many regions throughout the nuclear chart [1]. These isomers can generally be classified into groups depending on their nature. Three particularly common classifications are based on shape isomers, spin-trap isomers, and K isomers [1]. The mass A ~120–140 region of the nuclear chart, where ^{139}Eu lies, is of particular interest because nuclear behavior associated with several types of isomers have been observed there. For the lower-mass nuclei around A ~120, the protons populate the lower levels of the $Z = 50$ nuclear shell, whereas the neutrons populate the upper levels of the equivalent shell with $N \sim 74$–82. As a result of the reduced valance space near both of these closed shells, several isomers are found to exist (e.g., in the $^{124-130}_{50}$Sn nuclei [2]). With increasing mass, around $A \sim 140$, the proton Fermi surface lies amongst the lower-Ω prolate driving $h_{11/2}$ orbits and the neutron Fermi level lies around the higher-Ω oblate driving $h_{11/2}$ orbits. This prolate-oblate shape-driving competition for particular configurations can create the possibility for shape isomers to exist where the transitions linking these different nuclear shapes may be hindered (e.g., ^{144}Ho$_{77}$ [3,4], ^{142}Tb$_{77}$ [3,5,6], ^{140}Eu$_{77}$ [7], ^{134}Pm$_{73}$ [8], and ^{136}Pm$_{75}$ [9]). Finally, K isomers are also found in this mass region based on neutron number $N = 74$. K isomers occur where axially symmetric shapes are formed in the well-deformed midshell nuclei near the proton drip line (e.g., $^{136}_{62}$Sm, $^{138}_{64}$Gd, and $^{140}_{66}$Dy [10–13]). These K isomers are based on similar underlying Nilsson configurations to those K isomers established in the mass $A \sim 170$–180 region, with the $N = 74$ neutrons replaced by $Z = 74$ protons [1].

In some cases, the interpretation of the underlying configuration and classification of the isomers in the mass 120–140 region have been complicated. This is because a large fraction of these isomers decay by $E1$ transitions. Systematic studies of $E1$, $M1$, $E2$, and $M2$ transition probabilities have shown that $E1$ transitions between intrinsic states are often highly hindered compared with their single-particle Weisskopf or Nilsson estimates [14,15]. For example, the systematic studies of Lobner and Malmskog have revealed that $E1$ hindrance factors can span a range of 5 orders of magnitude from 10^{-7} to 0.01. These studies also found that the specific delay for any particular transition was not found to be a smooth function of nuclear mass, making interpretations based on systematic studies difficult [14,15].

The observation of an isomer in ^{139}Eu provides another example where the type of isomerism can be tested in the mass $A \sim 130$–140 region. At first sight, because ^{139}Eu has neutron number $N = 76$ and proton number $Z = 63$ it might be speculated that it is a well-deformed nucleus and perhaps that K isomerism may play a role. However, unlike in the $A \sim 170$–180 region [1], K isomers have rarely been established outside $N = 74$ in the $A \sim 130$–140 region [16]. Additionally, although ^{139}Eu has a β_2 deformation of 0.20, it has a gamma-soft configuration with nonaxiality parameter, $\gamma = +24^o$ [17]. Such γ softness would destroy the K quantum number and K-selection rule and would leave open the possibility that particular orbits could significantly influence the soft-nuclear shape. Transitions linking such differing nuclear shapes are often isomeric and for ^{139}Eu this, and the natural hindrance associated with configuration-changing $E1$ transitions, offers a likely explanation for the presence of the newly established 10(2)-μs isomer.

*Present Address: Department of Physics, Faculty of Engineering and Physical Sciences, University of Surrey, Guildford, GU2 7XH, UK.

†Present Address: Department of Physics, Oliver Lodge Laboratory, University of Liverpool, Liverpool, L69 7ZE, UK.

II. EXPERIMENT AND DATA ANALYSIS

High-spin states were populated in ^{139}Eu using a heavy-ion fusion-evaporation reaction. The K130 cyclotron at the Accelerator Laboratory of the University of Jyväskylä, Finland was employed to accelerate ^{54}Fe ions onto a $\sim$500-μg/cm^2 ^{92}Mo target at beam energies of 305 and 315 MeV. An average beam current of $\sim$6 pnA was used for 19 h at 305 MeV and 66 hours at 315 MeV. ^{139}Eu was populated weakly through the seven-particle ($5p2n$) exit channel. The ability to select such exotic reaction channels was possible by employing the high sensitivity and selectivity of recoil-isomer tagging [3–9,11,18–20] where prompt and delayed γ rays were correlated across isomeric states.

Prompt γ-ray decays were detected with 40 Compton-suppressed HPGe detectors of the JUROGAM target detector array with a total photopeak efficiency of $\sim$4% at 1.3 MeV [21]. Nuclear recoils were transported to the focal plane of the gas-filled recoil ion transport unit (RITU) [22] and implanted into a $\sim$500-μm thick aluminum foil. In the present experiment, recoil-isomer tagging was performed using a dual multiwire proportional counter (MWPC) setup which is described more fully in Ref. [5]. The use of a dual-MWPC setup allows larger recoil implantation rates to be accommodated in recoil-isomer tagging than with the standard setup where recoils are implanted into the GREAT double-sided silicon-strip detector [23]. Delayed γ-ray transitions from isomeric states were measured in the GREAT planar- and clover-germanium detectors close to the aluminum foil. Each decay was time stamped with a 100-MHz clock and recorded using the triggerless total data readout (TDR) system [24]. Data were sorted into two-dimensional matrices with GRAIN [25] and analysed with the UPAK [26] software packages.

III. RESULTS

The most intense delayed transitions observed with this reaction were from the known decay of an $\sim$300-ns isomeric state in ^{140}Eu through a $5p1n$ exit channel [7]. However, as a consequence of the short half-life of this isomer, most of the associated delayed radiation had decayed by $\sim$1 μs after each recoil implant at the focal plane. Analysis of the delayed focal plane spectrum, with a half-life condition that a delayed γ ray was detected more than 1 μs after a recoil implant, revealed the presence of a different series of low-intensity delayed γ-ray transitions of energies, 26, 117, and 122 keV and x rays of energy 40.9(2) and 47.2(2) keV from the electron conversion of the delayed γ rays. These x-ray energies are consistent with those expected for the 41.5- and 47.0-keV K_α and K_β x rays of Eu, respectively. Application of recoil-isomer tagging, revealed that the new delayed transitions were in delayed coincidence with a series of prompt transitions of energies 198, 471, 489, 582, 594, and 655 keV. A literature search revealed that the 26-, 117-, 122-, 198- and 489-keV transitions were established transitions in ^{139}Eu from the β-decay studies of the ground and isomeric states of ^{139}Gd [27]. The experimental method used in Ref. [27], detecting β-delayed transitions with a moving-tape system, would not have been sensitive to any short-lived μs isomers in the decays of the daughter nucleus, ^{139}Eu. In contrast, recoil-isomer tagging in the present work, reveals that some of the transitions established in Ref. [27] are in fact *delayed* as a result of a newly identified isomeric state in ^{139}Eu.

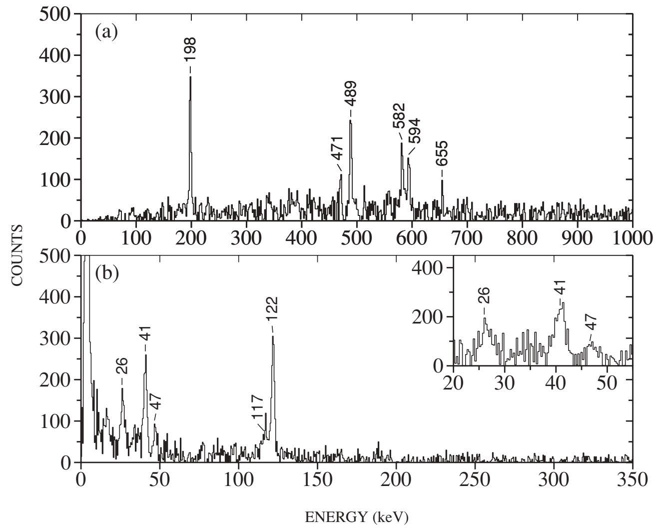

FIG. 1. Recoil-isomer-tagged spectra from a prompt-delayed matrix where the delayed γ rays were detected 1–33 μs after a recoil passed through the first MWPC. (a) Prompt JUROGAM spectrum showing the established 198- and 489-keV transitions in ^{139}Eu [27] along with the newly observed 471-, 582-, 594-, and 655-keV prompt transitions in ^{139}Eu from a single gate on the delayed 122-keV γ ray in ^{139}Eu. All labeled peaks have been assigned to ^{139}Eu. (b) Delayed planar spectrum showing the 26-, 117-, and 122-keV delayed transitions from a sum of gates on the prompt 198-, 489-, 582-, and 594-keV transitions in ^{139}Eu. The inset spectrum shows the low-energy region of this spectrum expanded for clarity. The 41- and 47-keV peaks are the K_α and K_β x rays of Eu, respectively.

Figure 1(a) shows the prompt spectrum obtained with recoil-isomer tagging on one of the delayed transitions, 122 keV. This spectrum reveals the presence of a series of prompt transitions of energy 198, 471, 489, 582, 594, and 655 keV. The 198- and 489-keV transitions were first established in Ref. [27]. Figure 1(b) shows the corresponding delayed spectrum obtained by setting gates on the prompt transitions (198, 489, 582, and 594 keV). These spectra were taken from a prompt versus delayed matrix which was constructed with the condition that the delayed decays were detected 1–33 μs after a recoil passed through the first MWPC. The first 0–1-μs range was avoided to suppress the strong contamination from the known $\sim$300-ns isomeric state in ^{140}Eu [7] and the matrix was background subtracted in time using delayed decays from the time interval 1–33 μs before a recoil was detected.

A. Measurement of the ^{139}Eu half-life

The half-life of the isomeric state in ^{139}Eu was determined from a series of focal-plane time spectra gated on the delayed 117- and 122-keV γ-ray transitions at both beam energies (see Fig. 2). The time parameter in this spectrum was defined as the time difference between a recoil passing through the first

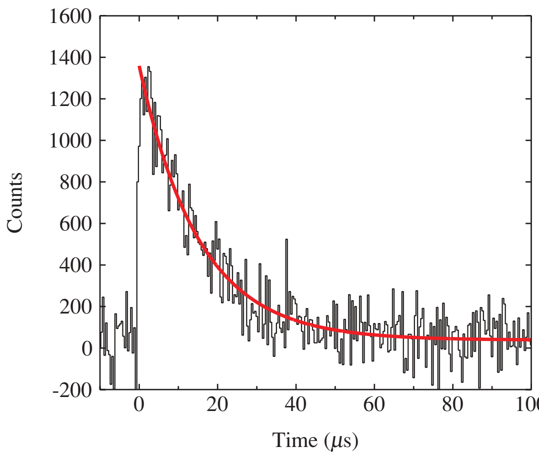

FIG. 2. (Color online) Time spectrum for the new 122-keV delayed γ-ray transition in ^{139}Eu. The "Time" axis label refers to the time difference between a recoil passing through the first MWPC and the detection of the delayed γ ray.

TABLE I. γ-ray energies, intensities, and initial and final spins for ^{139}Eu from the recoil-isomer tagged data in this work. The prompt and delayed intensities are normalized separately.

E_γ (keV)	I_γ	$J_i^\pi \rightarrow J_f^\pi$
	Delayed γ rays	
26.4(2)	34(6)	$(7/2^+) \rightarrow (9/2^-)$
40.9(2)	87(11)	K_α
47.2(2)	20(4)	K_β
117.2(1)	21(3)	$(13/2^-) \rightarrow (11/2^-)$
121.8(1)	100(11)	$(9/2^-) \rightarrow (11/2^-)$
	Prompt γ rays	
198.2(2)	86(13)	$(11/2^+) \rightarrow (7/2^+)$
470.7(4)	39(9)	$(27/2^+) \rightarrow (23/2^+)$
488.9(2)	100(10)	$(15/2^+) \rightarrow (11/2^+)$
582.3(7)	86(15)	$(19/2^+) \rightarrow (15/2^-)$
593.9(3)	66(13)	$(23/2^+) \rightarrow (19/2^+)$
655.2(4)	17(6)	$(31/2^+) \rightarrow (27/2^+)$

MWPC and a γ ray detected in the planar-Ge detector using the 100-MHz TDR clock. Using the TDR data, background was subtracted from these spectra using the 33-μs period prior to the arrival of a recoil at the focal plane. For each transition, half-life data were individually fitted with an exponential plus constant background term at each beam energy. (The individual half-life values and their statistical errors were 8.4(4), 10.7(2), and 11.9(5) for the 122-keV transition at 305 and 315 MeV and the 117-keV transition at 315 MeV, respectively.) The half-life of the isomeric state in ^{139}Eu was deduced from the mean and standard deviation of these individual half-life values to be 10(2) μs. The relatively large standard deviation with this limited sample size may suggest the presence of some unknown systematic error.

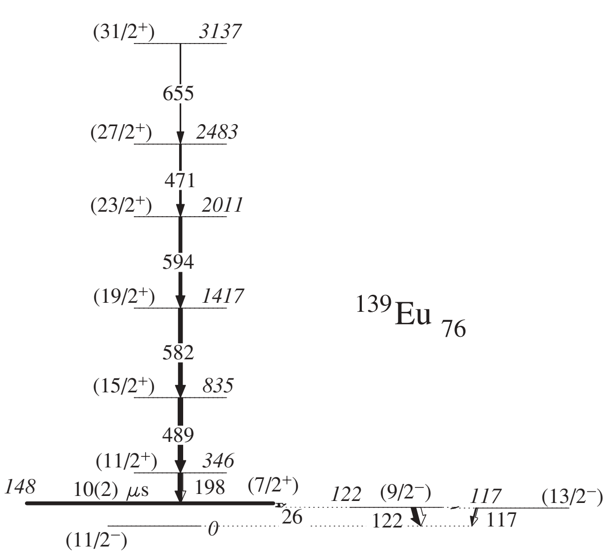

FIG. 3. Partial level scheme for ^{139}Eu showing the newly assigned 10(2)-μs isomeric state and the new 582-, 594-, 471-, and 655-keV prompt transitions. The 26-, 117-, 122-, 198-, and 489-keV transitions were first established in ^{139}Eu from the β-decay studies of the ground and isomeric states of ^{139}Gd [27]. The spins and parities of the states are discussed in Sec. IV A. The 117-keV transition was observed in the delayed spectrum from the isomer decay although the decay path to this state was not established in the present work (see text for details).

Figure 3 shows the partial-level scheme of ^{139}Eu deduced from this recoil isomer tagging study. The γ-ray energies and intensities deduced from the recoil isomer tagged spectra, shown in Figs. 1(a) and 1(b), are given in Table I. The ordering of the transitions above the isomer are based on their intensities as no γ-γ coincident information was available because of the limited statistics obtained in this experiment. The spin and parity assignments and the ordering of these prompt transitions will be discussed further in Secs. IV A and IV B, respectively. This level scheme is largely in agreement with that proposed in Ref. [27]. However, the state at excitation energy 148 keV was established in this work to have a half-life of 10(2) μs. In addition, the fact that the 117-keV transition is also observed in the delayed spectrum, Fig. 1(b), reveals that either there must be a link from this 148-keV isomeric state to the 117-keV state through a 30-keV transition, or that there must be a link from the state of excitation energy 122 keV to the state of excitation energy 117 keV through a 5-keV transition. Figure 1(b) does not show any evidence for a 30-keV transition which should have been observed with the level of statistics in this spectrum. However, the present setup would not have been sensitive to a 5-keV transition. Such a low-energy transition would need to penetrate through the stopper foil and thin Be window of the planar detector before it was detected. The efficiency for this process would be very small, and this may be the most-likely explanation why the delayed transition, which links into the 117-keV state, was not directly established in the present work [Fig. 1(b)].

IV. DISCUSSION

^{139}Eu has previously been the subject of several experiments [17,27–29]. The lowest members of the ground-state rotational band were first established from heavy-ion fusion-evaporation reactions [28]. Later, with improvements in detector efficiency, fusion-evaporation studies extended the ^{139}Eu level scheme by mostly populating yrast and near-yrast states up to high spins of around $47/2\hbar$ [17,29]. The nonyrast low-spin states of ^{139}Eu were identified from β-delayed studies of the 5.9(9)-s ground and 4.8(9)-s isomeric states of ^{139}Gd [27]. The present work has started to bridge the gap in knowledge between these yrast and nonyrast parts of the nuclear level scheme. Such studies are possible where (nonyrast) isomeric states can be used as a recoil-isomer tag with fusion-evaporation reactions. In the present work, a nonyrast rotational band was established built upon a 10(2)-μs isomeric state in ^{139}Eu. The properties of this band, and the γ-ray transition strength for the isomer decay, give information of the underlying single-particle configuration and the reasons for the isomerism of the level.

A. Spins and parities of the states

The spin and parity of the lowest state established in ^{139}Eu was assigned as $I^\pi = (11/2^-)$ in Refs. [17,27] and the 117-keV excited state was assigned as $I^\pi = (13/2^-)$ in Ref. [17]. In the present work, the spin and parities of the states fed from the isomer decay were deduced by consideration of the electron-conversion coefficients, total intensities, and Weisskopf single-particle half-life estimates for the transitions involved.

In this reaction, all of the K_α x-ray intensity shown in Fig. 1(b) is associated with the electron conversion of the 117- and 122-keV transitions. This is because the 26-keV transition energy is below the binding energy of the K shell. This information was used in conjunction with the γ-ray intensities from Table I to deduce the multipolarity of the delayed transitions. Electron-conversion coefficients have been calculated for each transition from the total intensity flow through each level and compared with the theoretical values tabulated in Ref. [30]. Assuming that the 117-keV transition is an $M1$ transition from Ref. [17], the experimentally calculated K_α electron-conversion coefficient for the 122-keV transition is $\alpha_K = 0.66(14)$. In comparison, the theoretical values for a 122-keV transition in ^{139}Eu from BRICC [30] are 0.88 for $M1$, 0.14 for $E1$, 6.7 for $M2$, and 0.68 for $E2$. From this comparison, the 122-keV transition is consistent with an $E2$ assignment within $\pm 1\sigma$ or with an $M1$ assignment within $\pm 2\sigma$. The possibility of any mixed $M1$ component to the 122-keV $E2$ transition would effectively be ruled out because the theoretical electron-conversion value for the $E2$ transition, 0.68, is already larger than the experimental value, 0.66(14). However, because of the relatively large uncertainty ± 0.14 on the experimental electron-conversion coefficient, some $M1$ mixing, up to 60% $M1$ and 40% $E2$, would still remain consistent with the current experimental value plus one standard deviation, 0.80. This cannot be ruled out in the present work and an experiment collecting higher statistics would be required to fully establish the extent of this potential mixing. The Weisskopf half-life estimates for a 122-keV transition are 12 ps for $M1$ and 0.48 μs for $E2$ multipolarity assignments, respectively. Both of these lifetimes would have been difficult to distinguish if they were convoluted with the decay of the 10(2)-μs isomer (Fig. 2). With the lack of any further information, the multipolarity of the 122-keV transition is assigned as an $E2$ transition in the present work.

Using similar methods, consideration of the total intensity flow for the 26-keV transition, relative to the newly assigned 122-keV $E2$ transition, reveals that the total electron-conversion coefficient for the 26-keV transition is 5.5(1.4). In comparison, the theoretical total electron-conversion coefficients for a 26-keV transition in ^{139}Eu from BRICC [30] are 13.7 for $M1$, 1.9 for $E1$, 725 for $E2$, and 1420 for $M2$. The experimental value is only consistent with a theoretical $E1$ assignment within $\pm 2.6\sigma$. The Weisskopf half-life for a 26-keV $E1$ transition is 15 ps, 0.6 ns for $M1$, and 972 μs for $E2$. The large half-life associated with an $E2$ transition would have been readily detected if it were convoluted with the decay of the 10(2)-μs isomer in Fig. 2 and this leaves the only possible assignments from the Weisskopf estimates to be $M1$ or $E1$. Combining this information with the electron-conversion analysis reveals that the most-likely transition multipolarity for the 26-keV transition is $E1$. The γ-ray transition strength for this 26-keV transition will be discussed in comparison with other $E1$ transitions in the neighboring nuclei in Sec. IV C.

The spin and parity of the isomeric state cannot be determined solely using the multipole assignments from the electron-conversion analysis. The electron-conversion analysis does not give information on whether the γ-ray transition carries away the full available angular momentum (stretched) or not (unstretched). This information is usually obtained from a directional correlation from the orientated states method. However, because the delayed transitions are observed at the RITU focal plane where the nuclear recoils have lost their initial alignment over several microseconds before the γ ray is emitted, this approach cannot be used. It can be argued that both the 122- and 26-keV γ rays cannot both be stretched transitions. This is because a stretched 122-keV $E2$ and a stretched 26-keV $E1$ transition assignment would lead to an isomer spin and parity of $(17/2^+)$ and the band built upon the isomer would form the yrast states in ^{139}Eu [17]. In this case, the new isomer band should have been readily observed in previous studies [17]. Because this was not the case, the new isomeric state was assigned a tentative $(7/2^+)$ configuration in the present work involving an unstretched 122-keV $E2(\Delta I = 1)$ transition and a stretched 26-keV $E1$ transition. This tentative assignment was guided by the properties of the band built upon the isomer (see Sec. IV B) and also upon the lowest available orbits around the proton Fermi surface in the theoretical calculations [17].

B. Aligned-angular momentum

The experimental aligned-angular momentum (or alignment), i_x, [31] for the band built on top of the new 10(2)-μs isomeric state in ^{139}Eu (solid squares) is shown in Fig. 4. A reference band with Harris parameters $\Im_o = 11\ \hbar^2/\text{MeV}$ and $\Im_1 = 10\hbar^4/\text{MeV}^3$ was subtracted [32]. These parameters were selected to give a flat aligned-angular momentum for

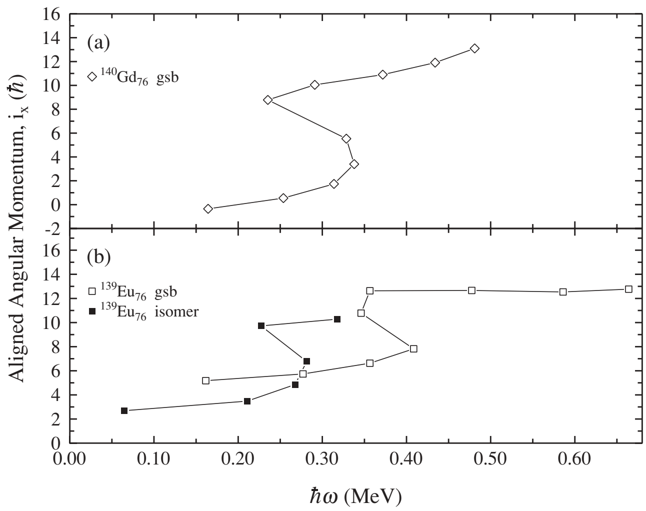

FIG. 4. Aligned-angular momentum for the ground-state bands in (a) ^{140}Gd [33], and (b) ^{139}Eu [17,28,29], and the new prompt band built upon the 10(2)-μs isomer in ^{139}Eu. Harris parameters $\Im_o = 11\,\hbar^2$/MeV and $\Im_1 = 10\,\hbar^4$/MeV^3 have been subtracted from each band in the figure.

the ground-state and isomer bands in ^{139}Eu at both low- and high-rotational frequencies. Also shown in this figure are the aligned-angular momentum for the ground-state band in ^{139}Eu (open squares) [17,28,29] and the ground-state band in $^{140}_{63}$Gd (diamonds) [33].

In this mass region, large gains in alignment observed near $\hbar\omega \approx 0.3$ MeV are understood to be from the lowest $h_{11/2}$ proton crossing, $\pi(ef)$. The lowest neutron $h_{11/2}$ configurations, $\nu(AB)$, are expected to align at a higher rotational frequency, $\hbar\omega \approx 0.5$ MeV [17,34]. For example, Fig. 4(a) shows that the ground-state band in even-even nucleus ^{140}Gd (diamonds) undergoes the first $\pi(ef)$ proton crossing at $\hbar\omega \approx 0.3$ MeV and the first, $\nu(AB)$, neutron crossing begins to occur at $\hbar\omega \approx 0.5$–0.6 MeV, although more data at higher rotational frequencies would be required to fully assign this crossing.

In contrast the ground-state band in the odd-proton nucleus ^{139}Eu [open squares in Fig. 4(b)] [17,28,29] does not show any gain in aligned-angular momentum at $\hbar\omega \approx 0.3$ MeV which is consistent with this first proton $h_{11/2}$ crossing being blocked in this band. This means that the configuration of the ground-state band in ^{139}Eu must involve at least one $h_{11/2}$ proton, in the e or f orbital. Because this is the ground-state band in ^{139}Eu, it must be the band built upon the lowest proton e orbital. The first band crossing observed in the ground-state band of ^{139}Eu occurs around $\hbar\omega \approx 0.37$ MeV and is associated with the first allowed proton crossing based on the $h_{11/2}$, $\pi(fg)$ crossing [17]. These observed crossings in ^{139}Eu are in good agreement with the theoretical cranked-shell-model calculations performed in Ref. [17].

For the newly established band built on top of the 10(2)-μs isomer in ^{139}Eu (solid squares) a gain in alignment is observed to occur at $\hbar\omega \approx 0.27$ MeV. This alignment gain and rotational frequency is quite similar to that observed in the ground-state band in ^{140}Gd [Fig. 4(a)] and is consistent with a crossing involving the lowest pair of $h_{11/2}$, $\pi(ef)$ proton orbitals in ^{139}Eu. The observation of this alignment in ^{139}Eu implies that the configuration of the newly established band on top of the isomer must not involve either of the lowest proton $h_{11/2}$ orbitals e or f. According to the theoretical cranked-shell-model calculations performed in Ref. [17], the next lowest orbits around the proton Fermi surface are based on the proton $g_{7/2}$ orbits. This and the estimated spins and parities of the bandhead isomeric state from the electron conversion analysis and the nonyrastness of the isomer, reveals that the most likely configuration for this new isomeric state in ^{139}Eu is based on a $\pi g_{7/2}$ orbit. The initial aligned-angular momentum for the isomer band at low rotational frequencies is about $\sim 3\,\hbar$. This is consistent with the proposed $g_{7/2}$ configuration of the isomer and the larger $\sim 5\,\hbar$ initial aligned-angular momentum of the $h_{11/2}$ ground-state band configuration in ^{139}Eu [see Fig. 4(b)].

C. γ-ray transition strengths and the lifetime of the isomeric state

The decay of the newly established isomer in ^{139}Eu takes place via a 26-keV $E1$ transition. The expected single-particle Weisskopf half-life, $t_{1/2}$(Weisskopf), for this 26-keV transition is 15 ps, which is much shorter than the 10(2)-μs experimental value, $t_{1/2}$(experiment). The large additional hindrance for the 26-keV γ-ray decay corresponds to a γ-ray transition strength [35] of

$$S = \frac{t_{1/2}(\text{Weisskopf})}{t_{1/2}(\text{experiment})} = 4.1(8) \times 10^{-6} \quad \text{W.u.},$$

using the Weisskopf single-particle estimate corrected for internal conversion. However, this small γ-ray transition strength actually lies well within the range expected from the systematic studies of Lobner and Malmskog for $E1$ transitions (10^{-7} to 0.01 W.u.) [14,15]. This may already suggest that the reason for the 10(2)-μs isomeric state in ^{139}Eu may just be a consequence of the natural hindrance associated with configuration-changing $E1$ decays.

To test these ideas further, the γ-ray transition strength for a series of $E1$ transitions in the neighboring odd-mass and even-mass nuclei in this region, those for the more neutron-rich Te isotopes near the closed shell [35] and those for the $N = 74$ K isomers in this region ^{136}Sm [36], ^{138}Gd [11], ^{140}Dy [12,13] are compared in Table II. In the table, the γ-ray transition strengths are grouped by the spin and parity of the initial state.

From Table II, it can be seen that the γ-ray transition strength for the new delayed 26-keV, $(7/2^+) \rightarrow (9/2^-)$, $E1$ transition in ^{139}Eu, $4.1(8) \times 10^{-6}$ W.u., is slightly larger than those of the other hindered-$E1$ decays in the neighboring odd-mass nuclei, ^{131}I, ^{147}Pm, and ^{149}Pm, $(1.4 - 2.6) \times 10^{-6}$ W.u. This larger transition strength reveals that the 26-keV, $E1$ transition in ^{139}Eu is less hindered than similar $E1$ decays in the neighboring nuclei. It is also evident from Table II that the γ-ray transition strength for the 26-keV decay in ^{139}Eu is also larger and less hindered than those of the $8^+ \rightarrow 7^-$ isomeric $E1$ decays in the neighboring even-even nuclei, ^{138}Pm to ^{148}Dy, $(0.1 - 2.2) \times 10^{-6}$ W.u. This may be understood because some of the isomeric states in ^{138}Pm to ^{148}Dy have been discussed in terms of shape isomers

TABLE II. γ-ray transition strengths for a series of $E1$ transitions grouped by the spin of the initial state, in the neighboring odd-mass and even-mass nuclei in this region from Refs. [35] and ^{142}Tb [5,6], ^{140}Eu [7], ^{144}Ho [3,4], ^{134}Pm [8], ^{136}Pm [9], ^{136}Sm [36], ^{138}Gd [11,37], and ^{140}Dy [12,13].

Nucleus	E_γ (keV)	Assigned multipolarity	$J_f^\pi \rightarrow J_i^\pi$	$t_{1/2}$ (ns)	γ-ray transition strength, S ($\times 10^{-6}$ W.u.)
^{139}Eu	26	$E1$	$(7/2^+) \rightarrow (9/2^-)$	$10(2) \times 10^3$	4.1(8)
^{149}Pm	270	$E1$	$7/2^- \rightarrow 7/2^+$	3.8(1)	1.4(1)
^{131}I	241	$E1$	$(15/2^-) \rightarrow (15/2^+)$	8.5(3)	1.6(1)
^{131}I	201	$E1$	$(15/2^-) \rightarrow (13/2^+)$	8.5(3)	2.6(1)
^{147}Pm	241	$E1$	$(11/2^-) \rightarrow (9/2^+)$	17(2)	1.4(2)
^{136}Sm	43	$E1$	$8^+ \rightarrow 7^-$	1500(100)	1.6(1)
^{138}Pm	174	$E1$	$8^+ \rightarrow 7^-$	21(5)	2.2(5)
^{140}Eu	98	$E1$	$8^+ \rightarrow 7^-$	299(3)	0.14(1)
^{142}Tb	37	$E1$	$8^+ \rightarrow 7^-$	$26(1) \times 10^3$	0.14(1)
^{144}Ho	57	$E1$	$8^+ \rightarrow 7^-$	519(5)	1.1(1)
^{148}Dy	95	$E1$	$8^+ \rightarrow 7^-$	95(30)	1.7(6)
^{128}Te	527	$E1$	$7^- \rightarrow 6^+$	3.47(4)	0.97(1)
^{130}Te	331	$E1$	$7^- \rightarrow 6^+$	166(12)	0.063(5)
^{132}Te	151	$E1$	$7^- \rightarrow 6^+$	$13(3) \times 10^3$	0.008(2)
^{134}Pm	71	$E1$	$(7^-) \rightarrow (6^+)$	$20(1) \times 10^3$	0.090(4)
^{136}Sm	466	$E1$	$8^- \rightarrow 8^+$	$15(1) \times 10^3$	0.00017(1)
^{138}Gd	583	$E1$	$8^- \rightarrow 8^+$	$6.2(2) \times 10^3$	0.00030(3)
^{140}Dy	574	$E1$	$8^- \rightarrow 8^+$	$6(1) \times 10^3$	0.00018(4)

(e.g., ^{144}Ho$_{77}$ [3,4], ^{142}Tb$_{77}$ [3,5,6], ^{140}Eu$_{77}$ [7], ^{134}Pm$_{73}$ [8], and ^{136}Pm$_{75}$ [9]). In these nuclei, isomers exist because particular nuclear configurations can influence and polarize the nuclear shape. This is particularly true for the prolate-driving-proton and oblate-driving-neutron $h_{11/2}$ orbitals involved in the isomeric- and ground-state configurations in these nuclei. However, in the $A \sim$ 130–140 region, the nuclear shapes are expected to be fairly soft with respect to nonaxial γ distortions [38]. This gamma softness and associated mixing of shapes may be the reason why the γ-ray transition strengths for the shape isomer decays of ^{144}Ho$_{77}$, ^{142}Tb$_{77}$, ^{140}Eu$_{77}$, ^{134}Pm$_{73}$, and ^{136}Pm$_{75}$ in Table II are not quite as small as might be expected if the isomer and ground states were based on more rigid-nuclear shapes.

In comparison, Table II shows that the γ-ray transition strengths for the $7^- \rightarrow 6^+$ transitions in the even-mass Te isotopes, ^{132}Te to ^{128}Te range from $(0.008–0.97) \times 10^{-6}$ W.u. As these tellurium isotopes have proton numbers close to the $Z = 50$ closed shell they may be expected to show single-particle nuclear behavior. As a consequence, these vibrational-like nuclei should have fairly rigid nuclear shapes and small γ-ray transition strengths. A similar γ-ray transition strength comparison can also be made with the K isomers in this region, ^{136}Sm [36], ^{138}Gd [11], ^{140}Dy [12,13] (see Table II). These well-deformed K isomers have fairly rigid prolate isomeric- and ground-state nuclear shapes with little nonaxial deformation ($\gamma \sim 0^o$). The γ-ray transition strengths for these K-isomer decays are very small on account of the large difference in K between the isomeric state ($K = 8$) and the ground-state band to which they decay ($K \sim 0$) [16] and the K selection rule governing the changes in K [1,14]. In stark contrast, the γ-ray transition strength for the 26-keV $E1$ transition in ^{139}Eu is four orders of magnitude larger or less hindered than these K-isomer decays.

In summary, the γ-ray transition strength for the 26-keV $E1$ transition in ^{139}Eu appears to be consistent with those of other shape-isomer decays in this region. This may be understood by the fact that the nuclear shape in ^{139}Eu is predicted to be gamma soft [17]. As a consequence of this softness, the isomeric nuclear shape based on the proton $g_{7/2}$ orbital may be expected to have a different nuclear shape to the ground state based on a proton $h_{11/2}$ orbit. It is this shape or configuration difference that is reasoned to result in the long-lived nature of the new $(7/2^+)$ 10(2)-μs isomeric state in ^{139}Eu.

V. CONCLUSIONS

A known state in ^{139}Eu was established to be isomeric from a recoil-isomer tagging experiment at the University of Jyväskylä. The properties of the new rotational band built upon this isomer reveal that is most likely based upon a $g_{7/2}$ configuration. The isomeric state decays via a 26-keV transition with a 10(2)-μs half-life whose internal-conversion coefficient is consistent with that of an electric-dipole transition. The γ-ray transition strength for the 26-keV $E1$ decay in ^{139}Eu was found to be similar to those of other isomeric-$E1$ decays in the neighboring nuclei. This comparison indicates that the hindered nature of the state in ^{139}Eu is most likely because of a difference in the nuclear shape between the isomeric $g_{7/2}$ state and the $h_{11/2}$ ground state to which it decays. A higher-statistics recoil-isomer tagging experiment focused on ^{139}Eu as the main exit channel would be beneficial to more fully establish configurations and alignments at higher rotational frequencies. In addition, the use of a differential plunger with recoil-isomer tagging would allow the lifetimes of the in-band transitions to be measured to define the deformation of the states in the isomeric band to compare with those of the ground-state rotational band.

ACKNOWLEDGMENTS

This work was supported by the European Union 6th Framework program, “Integrating Infrastructure Initiative-Transnational Access,” Contract No. 506065 (EURONS), and by the Academy of Finland under the Finnish Centre of Excellence Programme 2006–2011 (Nuclear and Accelerator Based Physics Programme at JYFL). The authors acknowledge the EPSRC/IN2P3 loan pool and GAMMAPOOL for the use of the JUROGAM detectors. P.J.R.M. and S.V.R. acknowledge receipt of EPSRC studentships. D.M.C. acknowledges the support of the STFC through Contract No. PP/F000855/1. C.S. (Contract No. 209430), P.T.G. (Contract No. 119290), and P.N. (Contract No. 121110) acknowledge the support of the Academy of Finland.

[1] P. Walker and G. Dracoulis, Nature (London) **399**, 35 (1999).
[2] R. L. Lozeva *et al.*, Phys. Rev. C **77**, 064313 (2008).
[3] C. Scholey *et al.*, Phys. Rev. C **63**, 034321 (2001).
[4] P. J. R. Mason *et al.*, Phys. Rev. C **81**, 024302 (2010).
[5] P. J. R. Mason *et al.*, Phys. Rev. C **79**, 024318 (2009).
[6] M. N. Tantawy *et al.*, Phys. Rev. C **73**, 024316 (2006).
[7] D. M. Cullen *et al.*, Phys. Rev. C **66**, 034308 (2002).
[8] D. M. Cullen *et al.*, Phys. Rev. C **80**, 024303 (2009).
[9] S. V. Rigby *et al.*, Phys. Rev. C **78**, 034304 (2008).
[10] A. M. Bruce, P. M. Walker, P. H. Regan, G. D. Dracoulis, A. P. Byrne, T. Kibèdi, G. J. Lane, and K. C. Yeung, Phys. Rev. C **50**, 480 (1994).
[11] D. M. Cullen *et al.*, Phys. Rev. C **58**, 846 (1998).
[12] D. M. Cullen *et al.*, Phys. Lett. B **529**, 42 (2002).
[13] W. Królas *et al.*, Phys. Rev. C **65**, 031303 (2002).
[14] K. E. G. Lobner, Phys. Lett. B **26**, 369 (1968).
[15] K. E. G. Lobner and S. G. Malmskog, Nucl. Phys. **80**, 505 (1966).
[16] A. M. Bruce, A. P. Byrne, G. D. Dracoulis, W. Gelletly, T. Kibèdi, F. G. Kondev, C. S. Purry, P. H. Regan, C. Thwaites, and P. M. Walker, Phys. Rev. C **55**, 620 (1997).
[17] P. Vaska *et al.*, Phys. Rev. C **52**, 1270 (1995).
[18] P. Mason *et al.*, Phys. Lett. B **683**, 17 (2010).
[19] D. M. Cullen *et al.*, in *International Conference on Frontiers in Nuclear Structure, Astrophysics, and Reactions—FINUSTAR 2, Crete, Greece. AIP Conf. Proc. 1012* (2008), p. 220.
[20] D. M. Cullen, in *AIP Conference Proceedings “Nuclear Physics and Astrophysics: From Stable Beams to Exotic Nuclei,” Cappadocia, Turkey. AIP Conf. Proc. 1072* (2008), p. 185.
[21] P. T. Greenlees *et al.*, Eur. Phys. J. A **25**, 599 (2005).
[22] M. Leino *et al.*, Nucl. Instrum. Methods Phys. Res., Sect. B **99**, 653 (1995).
[23] R. D. Page *et al.*, Nucl. Instrum. Methods Phys. Res., Sect. B: Beam Interactions with Materials and Atoms **204**, 634 (2003).
[24] I. Lazarus *et al.*, IEEE Trans. Nucl. Sci. **48**, 567 (2001).
[25] P. Rahkila, Nucl. Instrum. Methods Phys. Res., Sect. A **595**, 637 (2008).
[26] W. T. Milner, UPAK, The Oak Ridge Analysis Package, Oak Ridge National Laboratory, TN (private communication).
[27] X. Yuanxiang, X. Shuwei, L. Zhankui, Y. Yong, P. Qiangyan, W. Chunfang, and Z. Tianmei, Eur. Phys. J. A **6**, 239 (1999).
[28] S. Lunardi, F. Scarlassara, F. Soramel, S. Beghini, M. Morando, C. Signorini, W. Meczynski, W. Starzecki, G. Fortuna, and A. M. Stefanini, Z. Phys. A **321**, 177 (1985).
[29] P. J. Bishop, M. J. Godfrey, A. J. Kirwan, P. J. Nolan, D. J. Thornley, J. M. O’Donnel, R. Wadsworth, D. J. G. Love, and L. Goettig, J. Phys. G **14**, 995 (1988).
[30] T. Kibédi, T. W. Burrows, M. B. Trzhaskovskaya, P. M. Davidson, and C. W. Nestor Jr., Nucl. Instrum. Methods Phys. Res., Sect. A **589**, 202 (2008).
[31] R. Bengtsson and S. Frauendorf, Nucl. Phys. A **327**, 139 (1979).
[32] S. M. Harris, Phys. Rev. **138**, B509 (1965).
[33] E. S. Paul, K. Ahn, D. B. Fossan, Y. Liang, R. Ma, and N. Xu, Phys. Rev. C **39**, 153 (1989).
[34] E. S. Paul *et al.*, J. Phys. G: Nucl. Part. Phys. **19**, 861 (1993).
[35] P. M. Endt, At. Data Nucl. Data Tables **26**, 41 (1981).
[36] P. H. Regan, G. D. Dracoulis, A. P. Byrne, G. J. Lane, T. Kibédi, P. M. Walker, and A. M. Bruce, Phys. Rev. C **51**, 1745 (1995).
[37] M. G. Procter *et al.*, Phys. Rev. C (2010) (to be submitted).
[38] P. Moller, R. Bengtsson, B. Carlsson, P. Olivius, T. Ichikawa, H. Sagawa, and A. Iwamoto, At. Data Nucl. Data Tables **94**, 758 (2008).